

GIANT PALLADIUM CLUSTERS AS CATALYSTS OF OXIDATIVE REACTIONS OF OLEFINS AND ALCOHOLS

M. N. VARGAFTIK, V. P. ZAGORODNIKOV, I. P. STOLAROV, I. I. MOISEEV*

*N. S. Kurnakov Institute of General and Inorganic Chemistry,
Academy of Sciences of the U.S.S.R., Moscow 117907 (U.S.S.R.)*

D. I. KOCHUBEY, V. A. LIKHOLOBOV, A. L. CHUVILIN and K. I. ZAMARAEV*

*Institute of Catalysis, Siberian Branch of the U.S.S.R. Academy of Sciences,
Novosibirsk 630090 (U.S.S.R.)*

(Received August 10, 1988; accepted March 6, 1989)

Summary

Giant cationic palladium clusters approximated as $\text{Pd}_{561}\text{L}_{60}(\text{OAc})_{180}$ (L = phen, bipy) and $\text{Pd}_{561}\text{phen}_{60}\text{O}_{60}(\text{PF}_6)_{60}$ were synthesized and characterized with high resolution TEM, SAXS, EXAFS, IR and magnetic susceptibility data. The results of these studies suggest that L and O ligands are bound to Pd atoms located on the surfaces of close-packed metal skeletons of the clusters, while OAc^- and PF_6^- anions are outer-sphere ligands. Under mild conditions (293 - 363 K, 1 atm) the giant palladium clusters catalyze oxidative acetoxylation of ethylene into vinyl acetate, propylene into allyl acetate, and toluene into benzyl acetate; oxidation of primary aliphatic alcohols into esters; and conversion of aldehydes into acetals. Kinetics of oxidative acetoxylation of ethylene and propylene in solutions of the giant clusters were studied. A mechanism for these reactions is proposed, which includes the following steps: coordination of reagents by the cluster, oxidative addition of alkene to a Pd-Pd fragment and transfer of an electron pair from a Pd-H, Pd-vinyl, or Pd-allyl fragment to a coordinated molecule of oxidant (O_2 , peroxide, Pd(II)).

Introduction

Reduction of palladium(II) acetate with hydrogen in the presence of small quantities of 1,10-phenanthroline (phen) or 2,2'-bipyridine (bipy) followed by oxygen treatment gives rise to polynuclear palladium compounds (giant clusters) [1 - 3] which are catalytically active in various liquid-phase conversions of organic substances. In the present work, synthesis and structure as well as catalytic properties of the giant clusters are presented.

*Authors to whom correspondence should be addressed.

Experimental section

Preparation of [Pd₄phen(OAc)₂H₄]_n (n ≈ 100) polynuclear complex (1) [4]

A solution of 1.0 g (4.4 mmol) of Pd(OAc)₂ and 0.4 g (2.2 mmol) of phen in 100 ml of deoxygenated acetic acid was stirred under hydrogen at 293 K, 1 atm. After absorption of 1.3 mol H₂ per Pd atom, 500 ml of dry benzene were added under Ar. The precipitate was separated by decantation, washed with 3 × 100 ml of dry benzene, and dried under vacuum in Ar flow. Yield: 0.63 g (80% with respect to palladium). The substance 1 is a dark-brown, X-ray amorphous pyrophoric powder, soluble in water and polar organic solvents; under Ar it is stable at 293 K for several days. Found (%): C, 26.2; H, 2.05; N, 3.61; Pd, 59.0*. C₁₆H₁₈N₂O₄Pd₄: Calculated (%): C, 26.3; H, 2.46; N, 3.84; Pd, 58.6. High-resolution ¹H NMR (25 kHz frequency band, solutions in (CD₃)₂SO, CD₃OD, int. TMS) spectrum δ (ppm) = 1.9 - 2.1 (narrow singlet, OAc); 6 - 9 (poorly resolved multiplet, phen). ¹H NMR spectrum in 250 kHz frequency band (solution in CD₃CN): δ (ppm) = -53 (width 5 kHz). MAS ¹H NMR (solid sample) spectrum: δ (ppm) = -35.5; -38 (shoulder); -48. The number of [Pd₄Phen(OAc)₂H₄] units was estimated as approx. 100 on the basis of TEM and SAXS data (see below for details).

*Preparation of [Pd₉phen(OAc)₃]₆₀ cluster (2) [1, 2]***

A solution of 1 in acetic acid obtained as described above was stirred under oxygen at 293 K. After absorption of 0.5 mol of O₂ per gram-atom of Pd (10 - 20 min), the solution was filtered, and 500 ml of benzene was added to the filtrate. The precipitate formed was separated by centrifuging, washed repeatedly with benzene, and dried *in vacuo*. Yield: 0.57 g (85% with respect to Pd). The substance 2 is a dark-brown, X-ray amorphous powder with metallic luster, stable in air, and soluble in water and polar organic solvents. Found (%): C, 15.8; H, 1.1; N, 1.8; Pd, 69.6. C₁₈H₁₇N₂O₆Pd₉: Calculated (%): C, 16.4; H, 1.3; N, 2.1; Pd, 72.8. IR spectrum (film on KBr plate): 3040 (ν =CH), 2900 (ν -CH), 1560 (ν_{as} COO), 1395 (ν_s COO), 1126, 1087, 1025, 1000, 900, 825, 700, 633, 600 and 566 cm⁻¹. ¹H NMR (CD₃OD, int. TMS) spectrum: δ (ppm) = 2.0 (singlet OAc); 6 - 9 (unresolved multiplet, phen). The number of [Pd₉phen(OAc)₃] units was determined on the basis of molecular weight measurements, TEM and SAXS data (see below for details).

*Here and below the average values based on 10 - 15 parallel analyses are given. Absolute mean-square errors are (%): C, 1.3; H, 0.2; N, 0.4; Pd, 3.0.

**In the communications [5, 6], on the basis of preliminary data, the approximate formula [Pd₉phen(OAc)₃(O₂)₃]₆₀ was suggested for cluster 2. Subsequent refinement showed that [Pd₉phen(OAc)₃]₆₀ formula shows better agreement with the elemental analysis [1, 2].

Preparation of $[Pd_9phen(PF_6)O]_{60}$ cluster (3) [3b]

1.0 g (5.43 mmol) of KPF_6 in 100 ml of water was added to a solution of 0.5 g of cluster 2 in 200 ml of water. Just after mixing, a flaky precipitate is formed. After centrifuging, the precipitate was washed with 2×20 ml of ethanol and dried *in vacuo*. Yield: 0.55 g (90% with respect to palladium). The product was a dark-brown, X-ray amorphous powder with metallic luster, soluble in MeCN and mixtures of MeCN with acetic acid, insoluble in other organic solvents and water. Found (%): C, 11.9; H, 0.89; N, 2.1; F, 7.3*; Pd 72.5. $C_{12}H_8N_2OPF_6Pd_9$: Calculated (%): C, 11; H, 0.6; N, 2.1; F, 8.8; Pd, 73.7. IR spectrum: 830 cm^{-1} (ν PF). 1H NMR spectrum: δ (ppm) = 6 - 9 (unresolved multiplet, phen). ^{19}F NMR (CD_3CN , int. C_6F_6) spectrum: δ (ppm) = 71.3 (doublet, J (PF) = 708 Hz). The presence of O atoms in the formula for 3 has been argued on the basis of the stoichiometry of the substitution of OAc^- with PF_6^- anions, the metal core being unchanged (see later for details).

High resolution transmission electron microscopy (TEM)

These studies were carried out on a JEM-100 CX electron microscope with *ca.* 2 Å line resolution. TEM micrographs were obtained at the minimal electron beam intensities. The image scale was calibrated against the 3.345 Å interplanar distance of graphite. Samples for TEM study were prepared by pouring a drop of solution of substances 1, 2 or 3 in MeCN onto wholly carbon supports, followed by evaporation of solvent *in vacuo*. Since 1 is air-sensitive, samples were prepared and placed into the apparatus under an Ar atmosphere. In experiments with samples of 2, it was ascertained that transmission electron micrographs of each particular region of the support with clusters deposited on it gave virtually identical images for exposure times ranging from 10 s to 10 min.

Electron diffraction (ED) data

ED data were obtained for the same samples 1 - 3 deposited on wholly carbon films the same as those used in the TEM experiments; the same electron microscope was used. The exposure time was 1 to 3 min. When obtaining each diffractogram, an image region was chosen containing at least 10 - 20 palladium particles. Interplanar distances were calibrated against those for a film of crystalline gold photographed by the same apparatus in the same operating mode.

EXAFS data

EXAFS data for solid samples 1 - 3 were obtained with the use of synchrotron radiation from the storage ring VEPP-3 by techniques described elsewhere [7a, b]. Phase shifts, δ , for Pd-Pd and Pd-N distances were taken to be equal to the differences between the interatomic distances in

*Fluorine content was estimated on the basis of ^{19}F NMR spectra (CD_3CN , hexafluorobenzene internal reference) with an average error of 1.5% (absolute).

hypothetical molecules Pd₂ ($R = 2.70 \text{ \AA}$ for example) and PdN ($R = 2.00 \text{ \AA}$, for example) and positions of the RDA peaks for the model EXAFS spectra of these molecules, calculated according to [7a] using the phase and amplitude functions from [8]. The values of δ for compounds 1 - 3 were assumed to be the same as for the model diatomic molecules. This assumption is justified by the well-known fact of a rather weak dependence of δ on the oxidation states and actual atomic surrounding of the pair of atoms under consideration [8]. The Pd foil was used also as reference compound for receipt δ for the Pd-Pd distance and gave data similar to the model Pd₂ molecule.

Small-angle X-ray scattering (SAXS) data

SAXS data were obtained by a standard procedure [9] with the use of the small-angle X-ray chamber KRM-1.

NMR spectra

NMR spectra were recorded with Bruker WP-90 and CXP-300 spectrometers. Solid-state ¹H NMR spectra were obtained using a Bruker CXP-300 spectrometer with a magic angle spinning (MAS) adapter. The frequency of spinning was 2 kHz.

IR spectra

IR spectra were recorded with a Specord IR-75 (GDR) spectrometer in the range 400 - 4000 cm⁻¹.

Molecular mass

Molecular mass for cluster 2 was estimated from the rates of sedimentation in aqueous solution under ultracentrifuging with the use of a MOM-3180 (Hungary) ultracentrifuge at the maximum rate of rotation 58 000 s⁻¹. Molecular mass, M , was calculated on the basis of the Stokes-Einstein law, by the formula

$$M = \left(\frac{162\pi^2\eta_0^3 S_0^3 N_L^2 v}{(1 - v\rho_0)^3} \right)^{1/2},$$

where η_0 is viscosity of the solvent, S_0 is the 'true' (reduced to zero concentration of the solute) sedimentation coefficient; v is the partial specific volume of the solute; ρ_0 is the density of the solvent. The moving boundary method was applied using the same technique as that used in [10] for determination of sedimentation coefficients for the gold cluster.

Kinetic experiments

Kinetic experiments were performed at 313 - 363 K in continuous gas-flow (for reactions of ethylene, propylene) or in closed (for reactions of alcohols) thermostatic ($\pm 0.1 \text{ K}$) reactors shaken for minimization of the gas-liquid mass-transfer resistance. Reaction rates were followed by measuring

the accumulation of reaction products with GLC (Biochrom-1 chromatograph, USSR) and, for oxidation of alcohols, also by consumption of O_2 (gas-volumetric measurements). The experiments were performed at shaking frequencies 200 to 300 min^{-1} and gas flow rates 50 to 100 h^{-1} . The volume of the reactor was 10 ml. The volume of the liquid phase was varied from 2.0 to 4.0 ml. As we have shown in separate experiments, the rates of olefin oxidation were independent of shaking intensity, provided that the shaking frequency exceeded 100 min^{-1} , gas flow rate exceeded 50 h^{-1} , and the volume of the liquid phase in the reactor was in the range from 1.0 to 5.0 ml. Productivity of the reactor was found to be proportional to the volume of liquid phase. All these facts indicate a kinetic regime for the reactions studied.

Molar concentrations

Molar concentrations of olefins and O_2 in the solutions were calculated from the solubilities of these gases, determined by ordinary volumetric measurements.

Reuse of the catalysts

In a typical experiment (1 - 6 h), up to 10^4 moles of products per mole of the cluster (~20 moles per Pd atom) were obtained. After the oxidation of ethylene or propylene was completed, cluster 2 or 3 was precipitated from reaction solution by benzene or toluene, dried *in vacuo*, and then used in the next experiment. Three to four repeat experiments could be performed with a single sample of the cluster. Catalytic activity was slightly (10 - 30%) decreased after each experiment. The oxidation of alcohols (Table 7) was carried out as a heterogeneous reaction (alcohol in the liquid phase, cluster 3 as the solid phase) because of the insolubility of the cluster in alcohols. The cluster was filtered out after each experiment and was reused in repeat experiments without a noticeable decrease in catalytic activity.

Results and discussion

Preliminary observations

The oxidative acetoxylation of olefins catalyzed by palladium on inert supports in combination with alkali metal acetates at 420 - 470 K and 10 atm is well known [11 - 14]. We have found palladium black also to be active in this reaction under mild conditions (310 - 360 K, 1 atm) with the reactants in the liquid phase, provided that sodium acetate was brought into the reaction solution before reducing Pd(II) to Pd black, but not afterwards [15]. This observation led us to the conclusion that catalytic activity is provided by palladium atoms in some low oxidation state, rather than by palladium metal or Pd(II) [15].

However, transition metals are known to be stabilized in lower oxidation states typically by 'soft' bases such as π -acceptors (e.g. CO or phosphines) and heterocyclic N-bases with extended π -bond systems (e.g. bipy or phen) rather than by 'hard' bases such as CH_3COONa .

Carbonyl and phosphine complexes of Pt and Pd are unstable towards O_2 , especially in acidic media. Hence, we have chosen 2,2'-bipyridine and its derivatives (1,10-phenanthroline, 3,3'-dicarboxy-2,2'-bipyridine, 2,2'-bi-quinoline, etc.) as 'mild' bases, L, that could stabilize low oxidation states of palladium and at the same time are stable in the presence of O_2 and other oxidizing agents.

We have found [15, 16] that catalytically active solutions are formed via reduction of $\text{Pd}(\text{OAc})_2$, in the presence of the ligands L, with various reductants, the most convenient being H_2 . Catalytic activity for oxidation of olefins, as a function of total content of a 'mild' base L, exhibits an extreme pattern (Fig. 1).

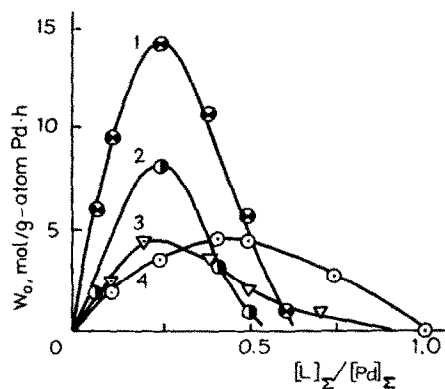


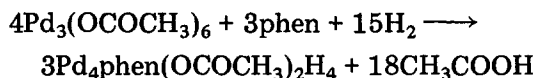
Fig. 1. The rates of ethylene and propylene oxidative acetoxylation (W_0) as functions of the $[\text{L}]_\Sigma/[\text{Pd}]_\Sigma$ ratio for the catalytic systems obtained by reduction of $\text{Pd}(\text{OAc})_2$ with hydrogen in AcOH solutions, for various ligands L. 333 K, 1 atm; 2:1 olefin: O_2 ratio in the gas phase. $[\text{L}]_\Sigma$ and $[\text{Pd}]_\Sigma$ are the total concentrations of L and Pd. (1) C_3H_6 , L = 2,2'-biquinoline; (2) C_2H_4 , L = 2,2'-dipyridine-3,3'-dicarboxylic acid; (3) C_2H_4 , L = 1,10-phenanthroline; (4) C_3H_6 , L = 1,10-phenanthroline.

Assuming the ratio $([\text{Pd}]_\Sigma/[\text{L}]_\Sigma)_{\text{max}}$ * to indicate the composition of the substance responsible for catalysis, one could arrive at the conclusion that ligand-deficient compounds of the cluster type catalyze the oxidation of olefins. In order to elucidate the nature of these compounds, we have studied the stoichiometry of the reactions leading to their formation, as well as their compositions and structures.

*Here $[\text{Pd}]_\Sigma$ and $[\text{L}]_\Sigma$ stand for the total concentrations of palladium atoms and L molecules in the solution, respectively, and the subscript 'max' denotes the value of the ratio corresponding to the maximum rate of olefin oxidation.

Polynuclear hydrides of palladium (1)

The primary isolated product of palladium(II) acetate reduction with H_2 in AcOH solution (containing 0.5 mol of phen per Pd atom) was an X-ray-amorphous substance with $Pd_4phen(OCOCH_3)_2$ as the simplest compositional formula, as ascertained by elemental analysis. However, as was found by volumetric measurement, H_2 consumption was 1.3 ± 0.05 mol per Pd(II) atom, corresponding to the stoichiometric equation:



The suggestion that the complex 1 is a hydride is supported by 1H NMR spectra [4]. In the $\delta = 0 - -80$ ppm region of the high-resolution spectrum (25 kHz frequency band), no signals from hydride atoms were detected for solutions of 1 in CD_3CN or CD_3OD , but in the broad-band spectrum (250 kHz frequency band), a wide line with a maximum at $\delta = -53$ ppm, in the region typical for hydride complexes, was revealed (Fig. 2). The same pattern was obtained for the solutions of the analogue of 1 containing bipy in place of phen. In the spectrum of the solid sample 1 registered with MAS technique, there are three slightly narrower (*ca.* 2 kHz) bands in δ interval -35 to -50 ppm (Fig. 2).

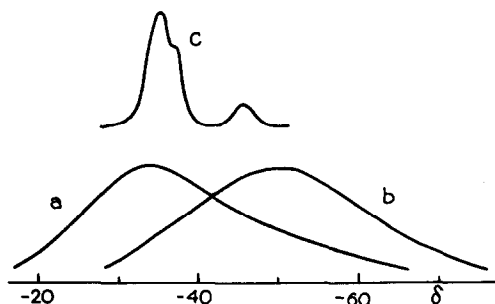


Fig. 2. 1H NMR broadband spectra of 1 in the hydride region: (a) solution of 1 in MeCN; (b) solution of the analogue of 1 (L = bipy instead of phen) in MeCN; (c) solid specimen 1 under magic angle spinning.

Considerable broadening of the hydride signal in the solutions spectra may be explained, *e.g.*, assuming that compound 1 is actually a rather large polynuclear palladium cluster, similar in its structure to a fragment of metallic palladium or its hydride phases. Note that a weak temperature-independent paramagnetism (specific susceptibility $\chi_g^{300} = 0.5 \times 10^{-6}$ CGSU) which is typical for metals indeed was detected for compound 1 in the temperature range from 77 to 300 K.

Protons of the CH_3COO groups of 1, in contrast to the hydride protons, were detected in the solution NMR spectra as a narrow signal with $\delta = 2.0$ ppm, while those of phen gave a broad unresolved multiplet in the range from 6 to 9 ppm. A considerable broadening of the usually well-resolved

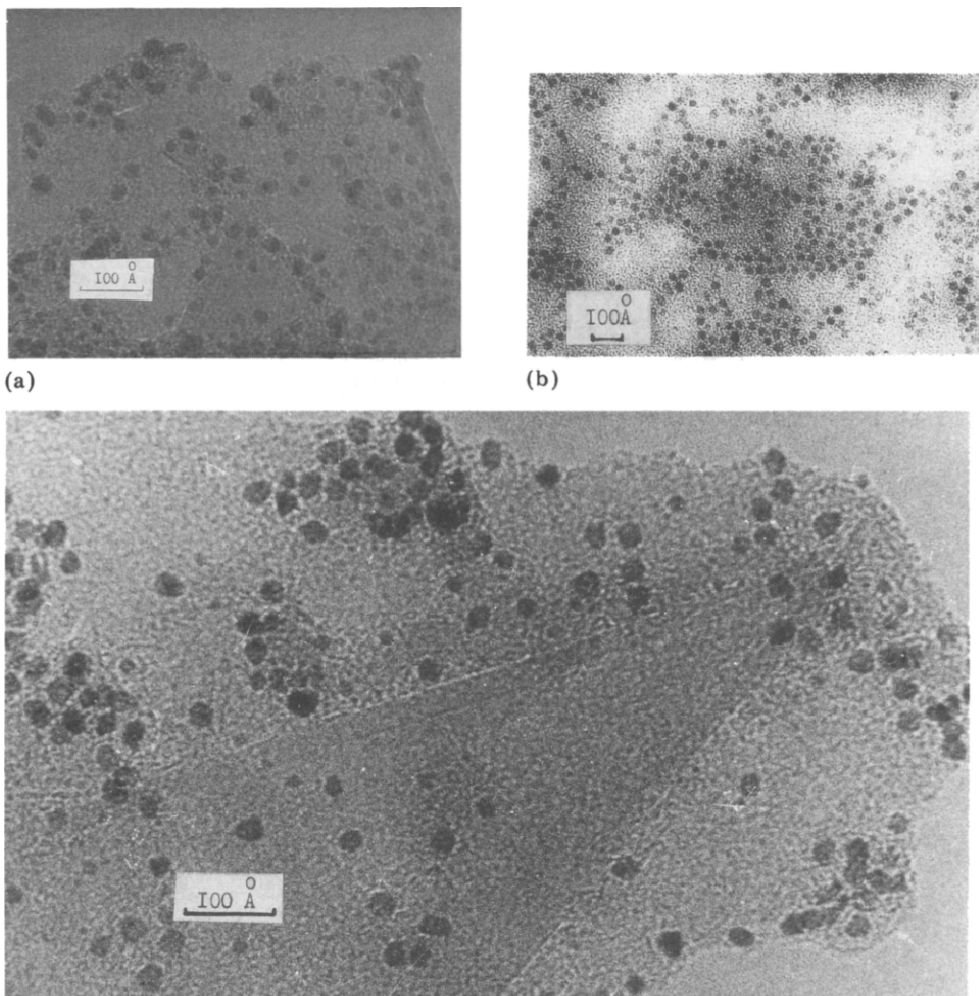


Fig. 3. TEM micrographs of the clusters: (a) 1; (b) 2; (c) 3.

multiplet of phen protons again can be explained by coordination of this ligand with Pd atoms of a large palladium cluster. The absence of such broadening in the case of the CH_3COO protons suggests that in solution acetate anions, in contrast to phenanthroline and hydride ligands, are not so tightly bound to the palladium cluster.

TEM (Fig. 3a) and SAXS (Fig. 4, curve 1) data showed that particles of 1 contain a metallic core of nearly spherical shape and of $20 \pm 5 \text{ \AA}$ in diameter. Note that both phen (bipy) and acetate ligands are invisible against the carbon support.

The function of radial distribution of atoms (RDA) obtained from EXAFS data [4] has a maximum, which, if attributed to the Pd-N bond, indeed corresponds to an interatomic distance $2.1 \pm 0.1 \text{ \AA}$, typical for Pd-N

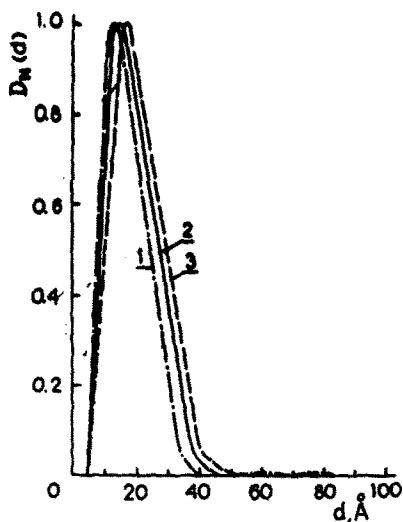


Fig. 4. Diameter distribution curves for the metal cores of clusters 1, 2 and 3 according to the SAXS data.

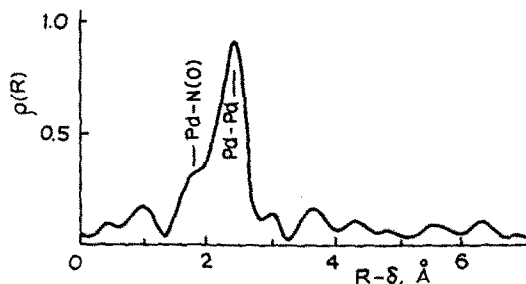


Fig. 5. RDA curve for cluster 1 obtained from EXAFS spectrum.

distances in palladium complexes [17], and a single peak for the shortest Pd-Pd distance, 2.6 ± 0.1 Å, which is noticeably smaller than the corresponding distance, 2.72 Å, for the bulk palladium metal (Fig. 5). Maxima corresponding to the distances between more remote palladium atoms were not detected, presumably as a result of some disorder in arrangement of palladium atoms, which could be induced by inclusions of hydrogen atoms in Pd skeleton of complex 1.

The metal core size for 1 molecules found from TEM and SAXS data allowed us to estimate the value of n in the idealized $[\text{Pd}_4\text{phen}(\text{OAc})_2\text{H}_4]_n$ formula as approximately 100, supposing the packing density of Pd atoms in 1 core to be nearly the same as that for bulk palladium metal. Additional experimental data (*e.g.* for Pd-Pd remote distances) are necessary for refinement of the n value and for determination of the packing of Pd atoms in 1 molecules.

The chemical properties of 1 testify to its high reactivity. As seen from Table 1, the action of various electrophilic reagents on 1 usually results in decomposition of 1 into oligomeric or mononuclear palladium complexes. In contrast, O_2 reacts with 1 and its analogues to yield a cluster with a massive, stable metallic skeleton.

Palladium-561 cluster (2)

When reacted with O_2 , compound 1 lost hydride atoms to form H_2O . In this process only a small portion of the Pd atoms was oxidized to Pd(II), while the majority of substance 1 was transformed into a polynuclear com-

TABLE 1

Predominant palladium-containing products formed in reactions of hydride complex 1 with various reagents at 293 K

Reagent	Solvent, reaction time	Product determined
Hg	CH ₃ COOH, 2 h	H ₂ , Pd amalgam
PPh ₃	DMFA, 3 h	H ₂ , Pd(PPh ₃) ₃
CO	1 atm, 1 - 3 h	[Pd ₄ phen ₃ (CO) ₃ H ₂ (OCOR) ₃] _n ^a R = Me, Et, t-Bu
NO	CH ₃ COOH, 1 h	Pd ₄ (NO) ₂ (OCOCH ₃) ₆
H ₂ NCON(Me)NO	DMFA, 24 h	Pdphen(NCO) ₂ [19]
tetrachloro- <i>o</i> -benzoquinone	DMFA, 3 h	(C ₆ O ₂ Cl ₄)Pd(Dmphen) ^b
phenH ⁺ X ⁻ , X = BPh ₄ , PF ₆ , AsF ₆	CH ₃ COOH, 1 - 3 h	Pdphen ₂ X ₂
O ₂	CH ₃ COOH, 10 - 30 min	[Pd ₉ phen(OCOCH ₃) ₃] ₆₀ (2)

^aOligonuclear hydride complex, $n \approx 2 - 3$ [18].

^bDmphen = 2,9-dimethyl-1,10-phenanthroline used in the analogue of 1 in place of phen [20].

pound 2 with Pd₉phen(OAc)₃ as the simplest formula, according to the elemental analysis data. The substance 2 is stable in air and soluble in water and polar organic solvents [1, 2].

The molecular mass of 2 was estimated as $(1.0 \pm 0.5) \times 10^5$ from data on sedimentation rates for 2 in aqueous solutions obtained by ultracentrifuge.

More accurate data on the size of the molecules of 2 were obtained by SAXS, TEM and electron diffraction [1, 2].

In TEM micrographs (Fig. 3b), metallic skeletons of 2 molecules were observed as nearly spherical particles 26 ± 3.5 Å in diameter. In the electron diffractogram of the same sample 2, there were several diffuse rings with arrangement of maxima close to those for the metallic palladium (see Table 2).

The nearly identical patterns of the interplanar distances found for 2 and for Pd metal might indicate the coincidence of the main symmetry features for the 2 metal skeleton with those of the fcc lattice for bulky Pd metal. However this suggestion contradicts the EXAFS data, which defi-

TABLE 2

Interplanar distances in the metal skeleton of 2 according to ED data

Substance	Interplanar distances (Å)				
2	2.26	1.95	1.39	1.17	0.89
Pd metal	2.23	1.94	1.37	1.17	0.89

nately indicate icosahedral packing of Pd atoms in 2 (see below). In this situation it seems more reasonable to assume that the similarity in the ED patterns of 2 and metallic Pd results from the destruction of 2 molecules to produce particles of metallic Pd under the influence of the electron beam. A destructive influence of the electron beam upon cluster molecules exposed in the electron microscope is indeed known to occur under the conditions of TEM and ED experiments. For example, the loss of cluster ligands, agglomeration and beam damage during TEM studies have been observed for $\text{Au}_{55}(\text{PPh}_3)_{12}\text{Cl}_6$ [21, 22] and $[\text{Ni}_{38}\text{Pt}_6(\text{CO})_{48}\text{H}](\text{NMe}_3\text{CH}_2\text{Ph})_5$ [23] clusters at high electron beam intensities and long experiment times. In our TEM experiments performed at low beam intensities, neither agglomeration nor beam damage of the shape of palladium clusters was found upon variation of the exposure time from 10 s to 10 min (see Experimental). However, total or partial loss of the cluster ligands cannot be excluded, even at the low beam intensities used. Ligand loss may result in a relaxation of the initial icosahedral metal skeleton into a fcc one (e.g. a cubooctahedron).

As mentioned above, no agglomeration of palladium particles was observed upon variation of the exposure time from 10 s to 10 min. In this situation, relaxation of the metal skeleton may be expected not to affect noticeably the size of the metal particles under investigation. If this is true, the electron diffractograms may be used for an independent estimation of the size of the metal core of 2 molecules. From the half-width of diffraction rings, the size of the particles responsible for the diffraction pattern was found to be *ca.* 25 Å, in agreement with TEM (Fig. 3b) and SAXS (Fig. 4, curve 2) data.

The consistency of the data on metal skeleton size obtained with various techniques (Table 3) seems to confirm the lack of considerable destruction of the metal skeleton or agglomeration of Pd clusters in our TEM and ED experiments. Note also that, as follows from the SAXS data, the size distribution of 2 cores is actually monomodal (Fig. 4).

TABLE 3

Metal skeleton size (*d*) of 2 molecules as evaluated by various techniques

Method	<i>d</i> (Å)
TEM	26 ± 3.5
ED	~ 25
SAXS	20 ± 5

The packing of Pd atoms in 2 was elucidated with EXAFS spectroscopy. The RDA curve characterizing the local environment of palladium atoms in 2 is given in Fig. 6. Using the well-known procedure for discrimination of the peaks due to atoms of light and heavy elements (see e.g. [7b]), one can distinguish in RDA the peaks corresponding to Pd–Pd distances and

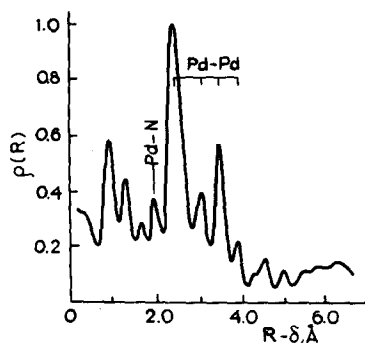


Fig. 6. RDA curve for cluster 2 obtained from EXAFS spectrum.

TABLE 4

The four shortest Pd—Pd distances in the metal skeleton of 2 found from EXAFS data, compared with these distances expected for various packings of Pd atoms

Data type	Pd—Pd distances (Å)			
EXAFS	2.60 ± 0.04	3.1 ± 0.1	3.66 ± 0.1	4.08 ± 0.1
packings ^a				
fcc	2.60	—	3.66	—
hcp	2.60	—	3.66	4.50
icosahedron	2.60	3.10	3.66	4.10

^aIn calculations, the shortest Pd—Pd distance was taken to be 2.60 Å for all packings; fcc = face-centered cubic packing; hcp = hexagonal close packing.

also find these distances. One of the peaks in the RDA curve of Fig. 6 was found to correspond to the distance 2.1 ± 0.1 Å between a Pd atom and a light N or O atom. The four other intense peaks correspond to the four shortest Pd—Pd distances (Table 4). The set of Pd—Pd distances obtained is seen to be consistent with the icosahedral packing of Pd atoms in the metal skeleton of the cluster 2 (the interatomic distance ratios expected for the four nearest neighbour atoms of the icosahedral skeleton are 1:1.2:1.4:1.6) and to deviate notably from the patterns of distances expected for fcc and hcp packings.

The mean atomic volume of Pd in the icosahedral metal skeleton of 2 calculated from the interatomic distances of Table 4 is *ca.* 16 \AA^3 , *i.e.* only slightly exceeding that of Pd metal (14.7 \AA^3). This result excludes the possibility of coordination of the cluster ligands phen and OAc by the inner Pd atoms. Therefore, the phen and OAc groups must be situated at the periphery of the metal core of cluster 2.

With the known character of packing of Pd atoms and the distances between the nearest neighbouring Pd atoms in the 2 core (Table 4), one can estimate the number of palladium atoms in cluster 2. As was found for a

sphere *ca.* 25 Å in diameter, the number, N_{Σ} , is approximately equal to 570. On the basis of this value for N_{Σ} and of the chemical composition of 2, suggested by the elemental analysis, the molecules of 2 may be approximated by the formula $\text{Pd}_{570 \pm 30} \text{phen}_{63 \pm 3} (\text{OAc})_{190 \pm 10}$. The molecular mass corresponding to this formula ($M = 83\,200$) agrees with the result of direct determination, by the rates of sedimentation in solution, of $M = (1 \pm 0.5) \times 10^5$.

The value found, $N = 570$, matches quite well the idealized 5-layer icosahedron containing, according to the formula [24] $N_{\Sigma} = 1/3 (10 m^3 + 15 m^2 + 11 m + 3)$, m (the number of layers) = 5, $N_{\Sigma} = 561$ metal atoms. Taking into consideration the chemical analysis, the overall $\text{Pd}_{561} \text{phen}_{60} (\text{OCOCH}_3)_{180}$ idealized formula can be suggested for the icosahedral cluster 2.

Thus we arrive at the conclusion that compound 2 is really a giant cluster containing more than 500 palladium atoms in its metal core. The idealized formula $\text{Pd}_{561} \text{phen}_{60} (\text{OAc})_{180}$ seems to correspond to some average size and composition of this cluster, rather than to a certain fixed size and composition. In other words, we anticipate the existence of distributions in the size and composition of various particles of 2, around the average value of $d \approx 25$ Å and the idealized composition $\text{Pd}_{561} \text{phen}_{60} (\text{OAc})_{180}$.

The following arguments can be presented in favour of this picture. First, as shown by Figs. 3 and 4, the metal cores of the particles of 2 are indeed characterized by a distribution over the values of their diameters, rather than by a single value of the diameter. This suggests that, in fact, various particles of the isolated substance 2 contain different numbers of palladium atoms in their cores. The situation here seems to resemble to some extent that for organic polymers, in which various molecules contain different numbers of monomer units. Second, taking into consideration that the average energy of Pd–Pd bonds is rather small (40 - 60 kJ mol⁻¹), the icosahedral metal clusters with $d \approx 25$ Å can be expected to have some defects ('caps', 'niches', etc.) which perhaps are not detected by TEM and other techniques used in this work.

Thus, the idealized formula $\text{Pd}_{561} \text{phen}_{60} (\text{OAc})_{180}$ indeed seems to represent some average picture of the particles having different sizes and, perhaps, also different chemical compositions. In a similar way, the model of an ideal icosahedral packing perhaps is just a first approximation of the actual structure. It seems that in reality we are dealing with a family of analogously constructed particles with predominantly icosahedral metal cores, and for this family it indeed seems appropriate to introduce the idealized average formula $\text{Pd}_{561} \text{phen}_{60} (\text{OAc})_{180}$, bearing in mind the comments given above.

Examination of molecular models shows that bidentately coordinated phen ligands, because of steric hindrances created by H atoms at their 2 and 2' positions, may be coordinated only at the edges and vertices of the icosahedron. At the outer layer of the idealized icosahedron which contains 252 metal atoms, in fact, *ca.* 60 bidentately coordinated phen ligands may

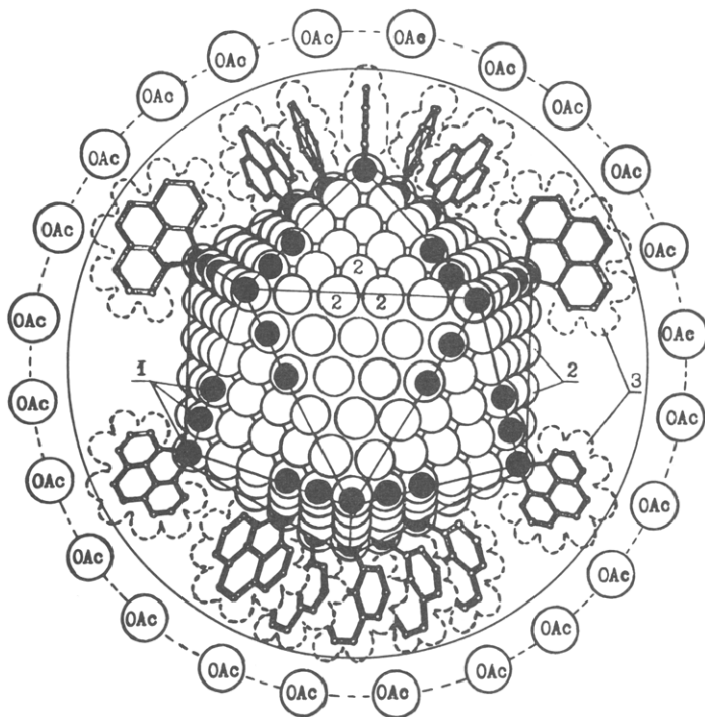


Fig. 7. Idealized model of cluster 2: 1 = Pd atoms coordinated with Phen ligands; 2 = Pd atoms accessible for coordination with OAc^- anions or molecules of substrates or solvent; 3 = van der Waals' shapes of coordinated phen molecules.

be arranged. Note also that the palladium core of 2 with icosahedral packing has a formal total charge of about +180, balanced by some 180 anion ligands.

With this arrangement, almost the whole surface of the metal skeleton is sterically screened by bulky phen ligands. Acetate anions may be located only in the outer sphere of cluster 2 (Fig. 7).

Note that a similar outer sphere arrangement of acetate anions was found also by X-ray structural analysis for the tetranuclear cluster $[\text{Pd}_4\text{phen}_4(\text{CO})_2](\text{OAc})_4$ with a tetrahedral metal skeleton [25] (Fig. 8).

The conclusion concerning the outer sphere coordination of CH_3COO ligands was confirmed by (1) IR spectra (the frequency difference $\nu_{\text{as}}(\text{OCO}) - \nu_{\text{s}}(\text{OCO}) = 165 \text{ cm}^{-1}$, i.e. as in CH_3COONa), by (2) data on electroconductivity of aqueous solutions of 2, and by (3) NMR spectra of 2, for which the line from the protons of OAc^- groups was observed as the usual narrow singlet with $\delta = 2.0 \text{ ppm}$, in contrast to the multiplet signal from the protons of phen that was noticeably broadened.

Palladium-561 cluster with hexafluorophosphate anions (3)

Cluster 2 can be precipitated from aqueous solutions by adding salts such as NaX or KX ($\text{X}^- = \text{Cl}^-$, Br^- , ClO_4^- , HSO_4^- , PF_6^- , AsF_6^-), with

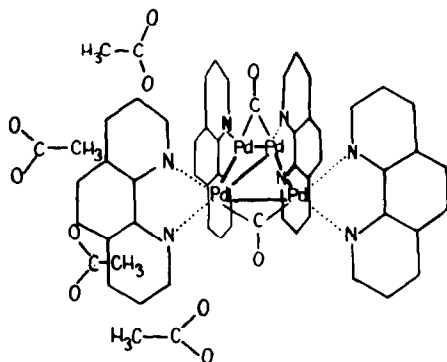


Fig. 8. The structure of $[\text{Pd}_4\text{phen}_4(\text{CO})_2](\text{OAc})_4$ cluster according to X-ray data [25].

substitution of OAc^- anions by X^- anions. Upon treatment of 2 with KPF_6 , a cluster soluble in CH_3CN , with idealized formula $\text{Pd}_{561}\text{phen}_{60}\text{O}_{60}(\text{PF}_6)_{60}$, 3, was obtained [3b].

The shape of the metal skeleton of cluster 3, as a TEM micrograph shows (Fig. 3c), is almost spherical, $28 \pm 5 \text{ \AA}$ in diameter, consistent with SAXS data (Fig. 4, curve 3).

Molecular clusters containing 4 - 38 palladium atoms are known to be diamagnetic [25, 26]. Unlike these, clusters 1 - 3, with several hundred Pd atoms in their cores, reveal metal-like properties such as temperature-independent paramagnetism (Fig. 9). The values of the specific magnetic susceptibility at 300 K ($\chi_g^{300} = 1.0 \times 10^{-6}$ CGSU for 2 and $\chi_g^{300} = 0.8 \times 10^{-6}$ CGSU for 3) are close to those for palladium particles supported on SiO_2 (dispersity 0.2 - 0.5, $\chi_g^{300} = (0.8 \pm 0.2) \times 10^{-6}$ CGSU) [27].

The metal core of cluster 3 was also studied by EXAFS (Fig. 10). An ordinary Fourier transform (FT) of the EXAFS spectrum of 3 (Fig. 10a) resulted in a RDA curve $\rho(R)$ with two maxima for Pd-Pd distances (Fig. 10b). The ratio of the two Pd-Pd distances, 1.4, tentatively suggests the fcc packing of Pd atoms in 3 [3a].

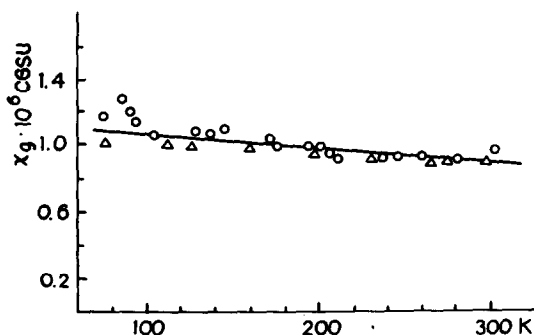


Fig. 9. Specific magnetic susceptibility, χ_g , of clusters 2 (○) and 3 (△) as a function of temperature.

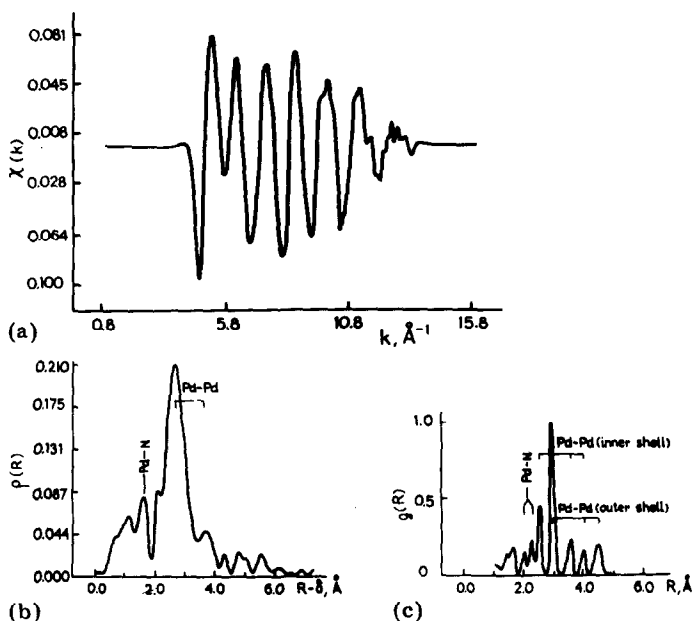


Fig. 10. EXAFS data for cluster 3: (a) EXAFS spectrum; (b) RDA curve from Fourier transformation of EXAFS spectrum; (c) RDA curve from statistical regularization procedure.

When determining the interatomic distances, R , from the positions, $R-\delta$, of the RDA peaks, the phase shift is $\delta = 0.22 \text{ \AA}$ for Pd–Pd distances and $\delta = 0.44 \text{ \AA}$ for Pd–light element distances. The values of δ were found as described in the Experimental section. The peak at 2.66 \AA for the shortest Pd–Pd distance of the $\rho(R)$ curve is essentially broader than two other significant peaks (3.70 \AA for Pd–Pd and 2.14 \AA for Pd–light atom distances). This suggests the presence of some unresolved ‘fine structure’ of the RDA curve. Note that we failed to reveal this ‘fine structure’ of the RDA curve via FT transform of the EXAFS spectra (Fig. 10a). We then used a statistical regularization (SR) method [28] for the analysis of the EXAFS spectrum. Usually this procedure gives better resolution than FT, and an *a priori* introduction of corrections for phase shifts, δ , is not necessary in this case, since the values of δ are obtained automatically with the SR procedure.

Figure 10b shows that the RDA function $g(R)$ calculated via SR agrees reasonably well with the RDA function $\rho(R)$ found with FT analysis. But the $g(R)$ curve is indeed better resolved, so that the ‘fine structure’ is clearly resolved, and the widths of all the peaks are small and almost identical [3b].

The set of interatomic distances obtained from the $g(R)$ function (Table 5) can be interpreted in terms of two different models. First, the set of Pd–Pd distances obtained from the $g(R)$ function might be attributed to a mixture of two clusters, one having an icosahedral metal skeleton like

TABLE 5

Interatomic distances, R , obtained by SR treatment of EXAFS spectrum of cluster 3

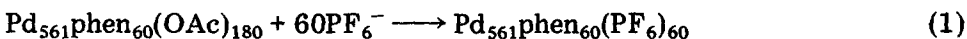
$R(\text{Pd-Pd}), \text{\AA} \pm 0.05 \text{\AA}$	2.55	2.95	3.6	4.05	4.45
$R(\text{Pd-light atom}), \text{\AA} \pm 0.1 \text{\AA}$	2.1	2.3			

that of 2 (with interatomic distances 2.55, 3.05, 3.60 and 4.05 Å), and the second having a fcc skeleton, probably in the shape of cuboctahedron, with Pd-Pd distances 2.95, 4.16, and 4.5 Å.

The shortest Pd-Pd distance $2.95 \pm 0.05 \text{ \AA}$ is typical for polynuclear Pd(II) compounds [17]. However, no admixture of Pd(II) was detected in solutions of cluster 3, e.g. by reaction with Γ^- ions. Moreover, the assumption that cluster 3 is a mixture, in comparable amounts, of two cluster species, one of which is built of Pd(II) atoms, hardly agrees with the observed values of magnetic susceptibility. All polynuclear compounds of Pd(II) are known to be diamagnetic [17]. Therefore, if substance 3 was a mixture of two clusters, only one component of this hypothetical mixture should be responsible for the observed paramagnetism of substance 3. In this situation it is difficult to explain why the values χ_g for clusters 2 and 3 are practically the same (Fig. 9) although cluster 3 contains both diamagnetic and paramagnetic particles, while cluster 2 contains only paramagnetic ones. Note also that quite similar size distribution curves were obtained for particles 2 and 3 from SAXS data (Fig. 4), which is also difficult to explain if cluster 2 contains only one type of cluster species, while cluster 3 contains two types of such species.

All the data mentioned above may be explained in a more consistent way in terms of another model, which implies that the product of the reaction 2 with KPF_6 is a rather uniform substance, similar in this respect to the initial cluster 2. Within this model, the EXAFS data should be treated as evidence of a more complicated arrangement of Pd atoms in 3 than in 2.

Let us discuss the charge balance for the reaction in which 2 is transformed to 3. Actually, a simple substitution of 180 OAc^- ions with 60 PF_6^- anions would leave a very large excessive positive charge of +120 on the

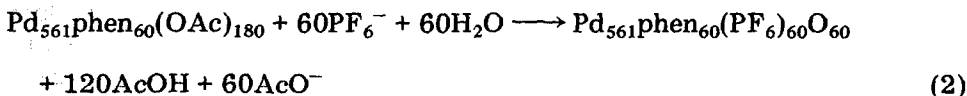


$\text{Pd}_{561}\text{phen}_{60}$ core. Thus we need some process that could balance this huge positive charge.

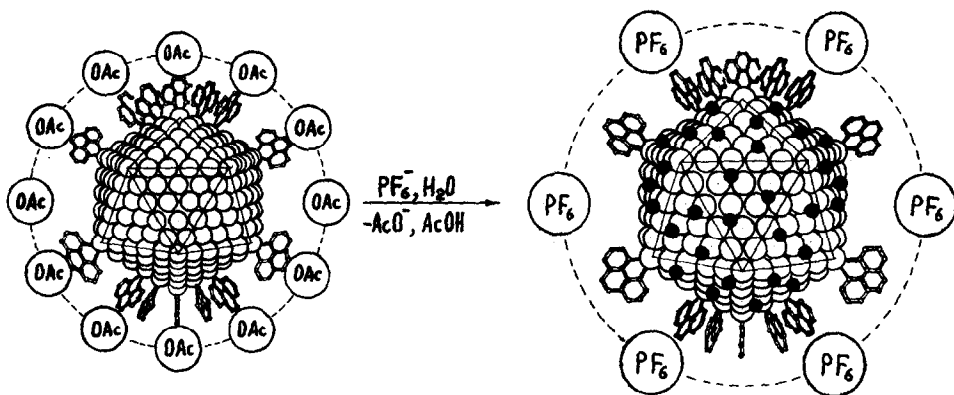
One such process might be a possible partial reduction of Pd atoms; however, there were no reducing agents in the reaction system. The hypothetical process (1) cannot be balanced by a redox disproportionation of palladium atoms, since no Pd(II) was detected in the reaction products, and the yield of 3 from 2, referred to Pd, was nearly 100%. Therefore, the core charge of cluster 3 is expected to be equal to that of cluster 2, and the ligand substitution process is assumed to include other anions besides PF_6^- . Perhaps the reaction is a hydrolysis resulting in the appearance of the anions

OH^- and O^{2-} at the cluster surface, accompanying the ligand substitution in aqueous solutions at pH 5 - 6. Unlike large PF_6^- and OAc^- anions, the small OH^- and O^{2-} anions can perhaps be bound directly to Pd atoms, rather than being located in the outer sphere of the cluster.

The content of C, H, N and Pd in the calculated composition of 3 is only slightly affected by inclusion of OH^- or O^{2-} in the formula of the cluster in an amount sufficient to balance the core charge upon the transition from 2 to 3. The lack of an absorption in the 3600 cm^{-1} region (which is characteristic of OH groups in the IR spectrum of 3) makes the O^{2-} anion a more likely hypothetical additional ligand:



Examination of molecular models shows that 60 oxygen atoms indeed can be coordinated as bridging groups at 20 faces of the 28 \AA icosahedron, with no steric hindrance to this coordination arising from 60 phen molecules. Thus, the transformation of cluster 2 to 3 can be presented as follows:



Scheme 1. ● = oxygen atom.

The oxygen ligands may also be inserted between two outer (*i.e.*, the 4th and 5th) icosahedral layers of Pd atoms. Both coordination of O atoms at the surface of the metal skeleton of 3 and their insertion between the outer layers of the skeleton are expected to lengthen the Pd-Pd distances in the outer layer. This can explain the appearance in the $g(R)$ function of cluster 3 of additional 4.45 \AA distance (Table 5) that does not fit the idealized icosahedral structure.

Thus, cluster 3 is inferred to be icosahedral, with the inner layers of its core being packed in the same way as those in cluster 2 (Pd-Pd distances are 2.55 , 3.05 , 3.60 and 4.05 \AA), and outer-layer Pd atoms (*ca.* 50% of total Pd) located at perturbed distances.

Note that the giant clusters obtained eventually serve as a bridge between ordinary molecular clusters and colloidal metals. The sizes of the metal skeletons of the giant clusters exceed notably those of large molecular clusters such as $\text{Pd}_{38}(\text{CO})_{28}(\text{PEt}_3)_{12}$ [26] and $\text{Au}_{55}(\text{PPh}_3)_{12}\text{Cl}_6$ [10], being close to lower sizes of colloidal metal particles. Unlike the latter, the giant clusters have a distinct ligand environment with a definite stoichiometry inherent in molecular clusters. However, a set of more or less imperfect metal polyhedra with a certain size distribution, rather than a single perfect polyhedron as in molecular clusters, seems to arise when the number of metal atoms amounts to several hundred. Nevertheless, the idealized formulae based on the data mentioned above are useful as models characterizing the average size and composition of the giant clusters and providing an understanding of their catalytic properties.

Catalytic activity of palladium clusters

Catalytic properties of cluster 1

Polynuclear hydride complexes of 1 type were found [4] to exhibit catalytic activity for hydrogenation of unsaturated compounds, dimerization of lower olefins, as well as positional isomerization of alkenes (Table 6). These reactions are typical for hydride complexes of transition metals as catalysts [29].

All these reactions are inhibited by oxygen, which converts 1 into the giant cluster 2, the latter having catalytic properties quite different from those of cluster 1.

TABLE 6

Reactions catalyzed by cluster 1 (acetic acid solution, 293 K, 1 atm)

Reaction	Reagent	Product	TN_{initial} (h^{-1}) ^a
hydrogenation	C_2H_4	C_2H_6	15
	$\text{PhCH}=\text{CH}_2$	PhC_2H_5	7
	$\text{CH}_2=\text{CHOAc}$	$\text{C}_2\text{H}_5\text{OAc}$	10
			12
dimerization	C_2H_4	C_4H_8	5
	C_3H_6	C_6H_{12}	0.3
isomerization	1- C_4H_8	mixture of n-butenes	10

^a TN_{initial} = initial turnover number calculated per Pd atom, determined at the beginning of the reaction (reaction times 0.2 - 0.5 h).

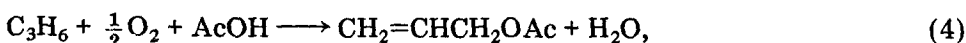
Catalytic properties of clusters 2 and 3

Acetoxylation reactions

In solutions of clusters 2 and 3 containing acetic acid, oxidative acetoxylation of olefins and alkylarenes occurs: ethylene is converted into vinyl acetate:



propylene into allyl acetate:



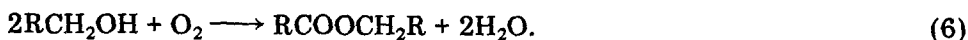
and toluene into benzyl acetate:



Selectivity of reactions (3) - (5) towards the products of oxidative acetoxylation is 95 - 98%. The only side reaction observed with these catalysts is subsequent oxidation of alkenyl and benzyl esters, when they are accumulated, to form ethylidene-, allylidene- and benzylidene diacetates, respectively. In comparison with metallic Pd catalysts, which show their activity at higher temperatures [11, 12], clusters 2 and 3 promote the side reactions to a lesser extent.

Oxidation of alcohols

In the presence of clusters 2 and 3, normal aliphatic alcohols are readily oxidized by dioxygen to form esters having the same carbon skeleton in both acid and alcohol components as the starting alcohol [30]:



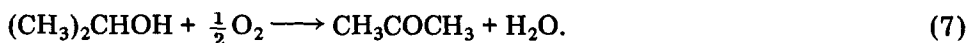
Besides esters, the oxidation of primary alcohols also yields aldehydes and their acetals (Table 7).

TABLE 7

Oxidation of alcohols by dioxygen (1 atm) catalyzed by cluster 3 (suspension of 0.1 g of 3 in 2.5 ml of alcohol)

Alcohol	Temperature (K)	$r_0 \times 10^3$ (mol h ⁻¹)	Products	Yield (%)
C ₂ H ₅ OH	333	2.3	CH ₃ COOC ₂ H ₅	27
			CH ₃ CHO	18
			CH ₃ CH(OC ₂ H ₅) ₂	55
n-C ₃ H ₇ OH	333	2.0	C ₂ H ₅ COOC ₃ H ₇	7
			C ₂ H ₅ CHO	77
			C ₂ H ₅ CH(OC ₃ H ₇) ₂	16
iso-C ₃ H ₇ OH	293	2.1	CH ₃ COCH ₃	100
n-C ₄ H ₉ OH	333	1.3	C ₃ H ₇ COOC ₄ H ₉	59
			C ₃ H ₇ CHO	3
			C ₃ H ₇ CH(OC ₄ H ₉) ₂	38

Secondary alcohols are smoothly oxidized into ketones:



In the absence of O_2 , the aldehyde added to the alcohol suspension of cluster 3 is converted into acetal:

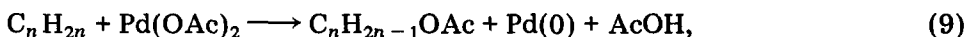


Thus, the giant clusters exhibit a variety of catalytic activities. As the first step in elucidating the nature of these activities, the kinetics of reactions (3) and (4) in solutions of the clusters were studied.

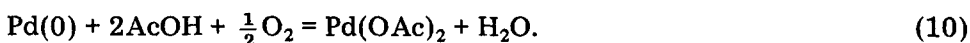
Kinetics and mechanisms of oxidative acetoxylation of ethylene and propylene in solutions of giant clusters

Oxidative acetoxylation of ethylene and propylene via reactions (3) and (4) is known to be carried out homogeneously in solutions of AcOH containing Pd(II) + OAc^- ions [31], and heterogeneously in the presence of metallic palladium combined with alkali metal acetates [11 - 14]. Heterogeneous acetoxylation reactions can be performed with both liquid and gas phase reactants.

In solutions of Pd(II), the reaction involves oxidation of olefin by palladium(II):



followed by regeneration of Pd(II) from Pd(0) under the action of O_2 :



When obtaining vinyl and allyl acetates with solid catalysts under oxygen + acetic acid vapour at 430 - 470 K [11, 12, 14], oxidation of metallic palladium to form Pd(II) may, in principle, occur. However, the thermal instability of Pd(II) acetate complexes at temperatures above 373 K, as well as the data on selectivity of reactions (3) and (4) in systems including Pd(II) [16, 32, 33], contradicts the hypothesis of the heterogeneous process via reactions (9) and (10).

In the case of $\text{Pd}(\text{OAc})_2$, interaction with propylene in liquid AcOH, a mixture of allyl, isopropenyl and n-propenyl acetates is formed. The allyl acetate yield decreases with increasing temperature up to 380 K and aqueous contents of the solution up to 1 - 3%, at the expense of acetone yield increase. Over Pd metal catalysts, the noted side products are not actually formed, and almost no decrease in the yield of allyl acetate is observed upon a temperature increase from 420 to 460 K and addition of water up to 10%.

In the case of ethylene, both in heterogeneous and homogeneous systems, the same ester, vinyl acetate, is formed. However, in Pd(II) systems, even small (0.2 - 1.0%) quantities of H_2O result in the appearance of acetaldehyde, whereas in the case of Pd metal catalysts, vinyl acetate is the sole product of the oxidation of ethylene even at significantly higher water contents [15, 36].

For oxidation of alkyl arenes in the presence of carboxylic acids, substantial differences in selectivity of homogeneous Pd(II) and heterogeneous Pd metal catalysts are also observed. For example, under the action of Pd(II), toluene is converted mainly into bitolyls, which are the products of oxidative coupling of aromatic rings. Over metallic Pd in the presence of RCOOH, oxidative carboxylation of the methyl group becomes the main route of toluene oxidation [34]:



From the above data, it follows that in systems where both Pd(II) and Pd metal are present, vinyl and allyl acetate can be formed by two different routes. The mechanism of the route with participation of Pd(II) has been investigated in detail [31, 35], whereas the mechanism of the route with participation of Pd metal, in spite of some kinetic studies [36], is still not clear. In particular, it remains unknown in what stages the reagents are activated and via what path their conversion at a metal surface proceeds.

Our experiments showed that only vinyl and allyl acetates were formed by ethylene and propylene oxidations, respectively, in solutions of clusters 2 and 3 containing up to 10% H₂O. The fact that carbonyl compounds are absent from the products seems to exclude the possibility that the reactions occur via oxidation of some of the cluster Pd atoms to Pd(II) and subsequent reduction of Pd(II) by olefins, *i.e.* via reactions (10) and (9). Therefore, clusters 2 and 3 may be regarded as good models of solid catalysts for which, in contrast to homogeneous Pd(II) systems, the selectivity of olefin oxidation is rather insensitive to the presence of water.

Kinetics of ethylene and propylene oxidation. Cluster 2 is soluble in AcOH and in its mixtures with diglyme, while cluster 3 can be dissolved in MeCN–AcOH mixtures. Therefore, the kinetics of reaction (3) were studied in MeCN–AcOH solutions of cluster 3, and those of reaction (4) both in MeCN–AcOH solutions of cluster 3 and in diglyme–AcOH solutions of cluster 2. The concentration of AcOH in these mixtures was varied in order to determine the reaction order with respect to AcOH.

In a flow reactor with gaseous olefins and O₂ at a constant flow rate of ethylene + oxygen mixture and constant concentration of acetic acid in the solution, the observed rate of vinyl acetate formation, r_0 , was found to increase as a linear function of the concentration of cluster 3 in the interval from 2.4×10^{-5} to 1.77×10^{-4} M (Fig. 11).

The observed first-order rate constant, k_{obs} , increased nonlinearly with increasing concentrations of ethylene, oxygen and acetic acid. The dependences of k_{obs} on these concentrations are represented by saturation kinetics, with straight lines when the data are plotted according to a linearized form of the Michaelis–Menten equation (Figs. 12–14). Thus, experimental values for the reaction rate may be described by the rate equation [37]:

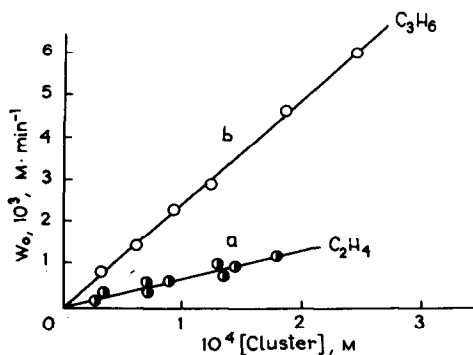


Fig. 11. Dependence of the initial rate (r_0) on the concentrations of cluster 3 for reactions (3) (a) and (4) (b). 333 K; solvent MeCN–AcOH mixture; for ethylene oxidation $[\text{AcOH}] = 1.59 \text{ M}$, $[\text{C}_2\text{H}_4] = 2.16 \times 10^{-2} \text{ M}$; for propylene oxidation $[\text{AcOH}] = 1.75 \text{ M}$, $[\text{C}_3\text{H}_6] = 9.0 \times 10^{-2} \text{ M}$.

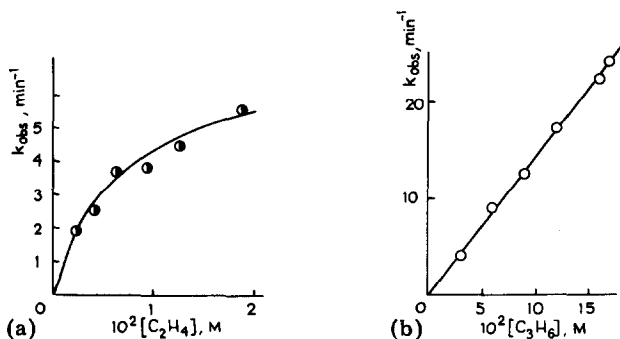


Fig. 12. The observed rate constant, k_{obs} , for formation of vinyl acetate (a) and allyl acetate (b), as functions of the ethylene and propylene concentrations. 333 K, solvent MeCN–AcOH mixture, $[\text{AcOH}] = 1.59 \text{ M}$, $[\text{O}_2] = 4.2 \times 10^{-3} \text{ M}$, $[\text{3}] = 1.25 \times 10^{-4} \text{ M}$.

$$r_0 = k[\text{cluster}] \frac{[\text{C}_2\text{H}_4][\text{O}_2][\text{AcOH}]}{(K_{\text{I}} + [\text{C}_2\text{H}_4])(K_{\text{II}} + [\text{O}_2])(K_{\text{III}} + [\text{AcOH}])} \quad (12)$$

where [cluster] stands for the concentration of the giant cluster.

The rates, r_0 , of allyl acetate formation from propylene in solutions of both cluster 2 and cluster 3 are also proportional to the concentrations of the latter (Fig. 11). But for propylene oxidation, in contrast to ethylene oxidation, the dependence of r_0 on the concentration of C_3H_6 demonstrates no deviation from linearity (Fig. 12b). The influence of the concentration of acetic acid on r_0 for C_3H_6 oxidation is described by Michaelis–Menten kinetics (Fig. 13).

With the oxygen concentration being varied, the variations in the reaction rate for propylene oxidation are more intricate than for ethylene oxidation. Under 0.9 atm of C_3H_6 partial pressure, this function looks like the curve with saturation. However, under 0.5 atm of propylene in the $r_0 =$

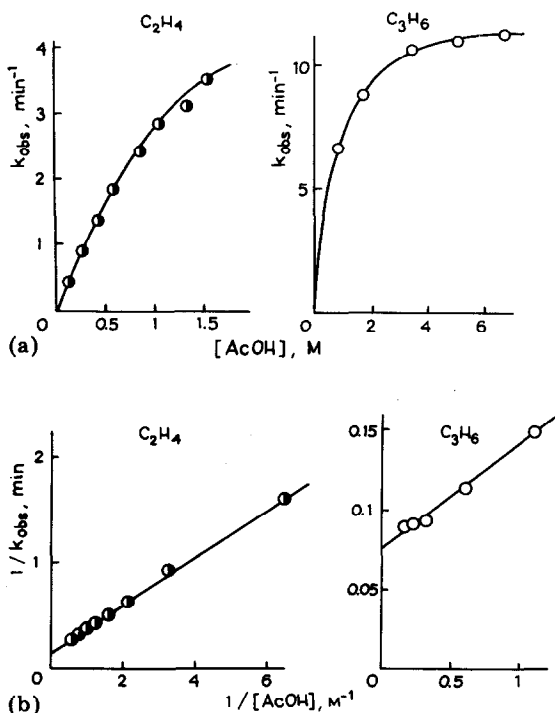


Fig. 13. The values of k_{obs} as a function of AcOH concentrations for ethylene (●) and propylene (○) oxidations; (a) the same data in Michaelis-Menten coordinates; (b) 333 K, solutions in MeCN-AcOH mixtures, $[\text{O}_2] = 4.2 \times 10^{-3}$ M; for (●) $[\text{C}_2\text{H}_4] = 2.16 \times 10^{-2}$ M; $[\text{I}] = 1.09 \times 10^{-4}$ M; for (○) $[\text{C}_3\text{H}_6] = 9.0 \times 10^{-2}$ M, $[\text{I}] = 1.25 \times 10^{-4}$ M.

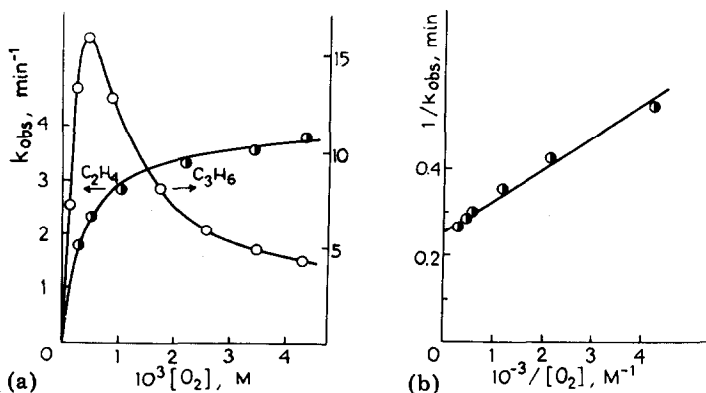


Fig. 14. Dependence of k_{obs} on the O_2 concentrations for ethylene under $P(\text{C}_2\text{H}_4) = 0.2$ atm and propylene under $P(\text{C}_3\text{H}_6) = 0.5$ atm; (a) the same data in Michaelis-Menten coordinates; (b) 333 K, solvent MeCN-AcOH mixtures; for C_2H_4 oxidation $[\text{AcOH}] = 1.59$ M, $[\text{C}_2\text{H}_4] = 2.16 \times 10^{-2}$ M, $[\text{I}] = 1.09 \times 10^{-4}$ M; for C_3H_6 oxidation $[\text{AcOH}] = 1.75$ M, $[\text{C}_3\text{H}_6] = 0.162$ M $[\text{I}] = 1.25 \times 10^{-4}$ M.

TABLE 8

The constants of the kinetic equation (12) at 333 K

Substrate	Cluster	k (min^{-1})	$K_I \times 10^3$ (mol l^{-1})	$K_{II} \times 10^4$ (mol l^{-1})	K_{III} (mol l^{-1})
ethylene	3	8.2 ± 0.7	5.8 ± 0.3	3.0 ± 0.2	1.3 ± 0.1
propylene	3	3.3 ± 0.3	≥ 30	5.2 ± 0.3	0.67 ± 0.05
propylene	2	5.6 ± 0.5	≥ 30	1.2 ± 0.1	4.8 ± 0.5

$f(P_{O_2})$ function there appears a maximum (Fig. 14). The decrease in r_0 upon increasing P_{O_2} above a certain value, corresponding to the maximum of r_0 , suggests an inhibition of the reaction by O_2 under low pressure of C_3H_6 . Under high enough pressures of C_3H_6 , ($P_{C_3H_6} \geq 0.7$ atm) inhibition of the reaction is imperceptible, and the rate of the propylene oxidation is described by an equation similar to eqn. (12) [38].

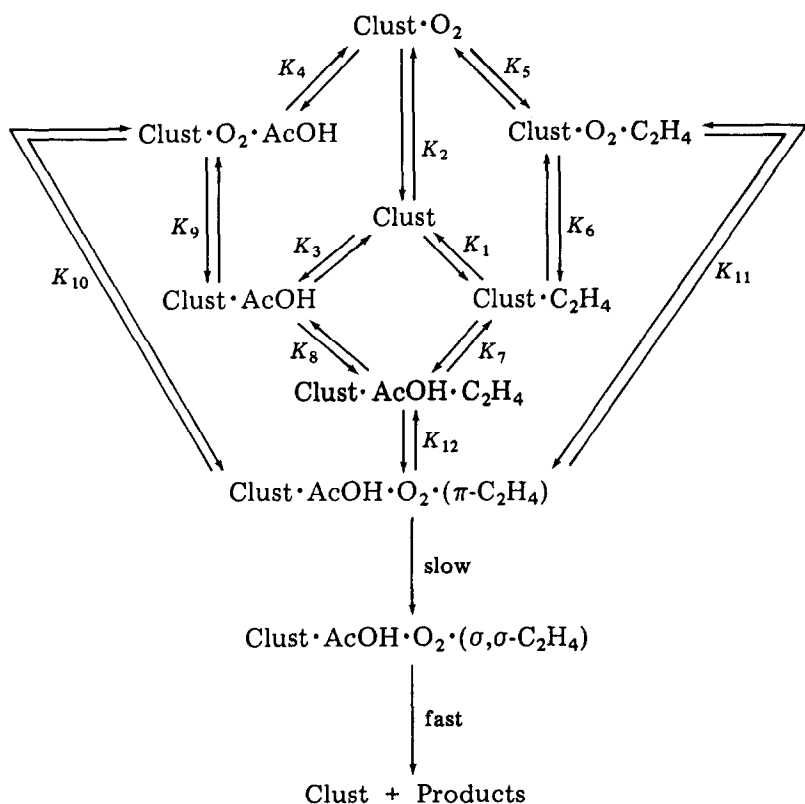
From Table 8 it is seen that the rate constants, k , for ethylene and propylene oxidations in solutions of both clusters differ less than three-fold. The Michaelis constants K_I , K_{II} and K_{III} for both olefins are also of the same order of magnitude, the largest variation upon the change of the olefin being observed for the constant K_I . The Michaelis-Menten character of the kinetics of reactions (3) and (4) suggests the product formation to be preceded by stages of reversible coordination of olefin, O_2 and AcOH molecules with the cluster. A comparison of the values of K_I (Table 8) shows propylene to be coordinated notably more weakly than ethylene and O_2 .

In homogeneous oxidation of olefins with Pd(II), the products of the oxidation appear, in the absence of dioxygen, in stoichiometric quantities with respect to that of the Pd(II) reacted. In contrast, in the case of clusters 2 and 3, the oxidation of olefins in the absence of dioxygen is not observed. This fact further supports the conclusion that reactions of ethylene and propylene in the presence of the giant clusters cannot be explained by alternating oxidation-reduction reactions of the cluster with substrate and oxidant molecules. The kinetic data obtained can be explained in terms of the reaction mechanism shown in Scheme 2.

Under steady-state conditions the expression for the reaction rate, r_0 , that corresponds to this mechanism is as follows:

$$r_0 = \frac{kK_3K_9K_{10}[\text{Clust}][\text{Ol}][O_2][\text{AcOH}]}{\{1 + K_1[\text{Ol}] + K_2[O_2] + K_3[\text{AcOH}] + K_2K_4[\text{AcOH}][O_2] + K_2K_5[\text{Ol}][O_2] + K_3K_8[\text{AcOH}][\text{Ol}] + K_2K_4K_{10}[\text{Ol}][O_2][\text{AcOH}]\}} \quad (13)$$

where [Clust] and [Ol] stand for the concentrations of a giant cluster and an olefin, respectively. Note that the reaction between the coordinated C_nH_{2n} , O_2 and AcOH species characterized by the effective rate constant



Scheme 2.

k , is expected to be in fact a complex one, consisting of several elementary steps.

Equation (13) may be represented in the same form as the experimental equation (12) provided that: $K_{\text{I}} = 1/K_1$, $K_{\text{II}} = 1/K_2$, $K_{\text{III}} = 1/K_3$, $K_1 = K_8$, $K_3 = K_4$ and $K_2 = K_5 = K_{10}$, that is, when the stability constants for the complexes formed by cluster 2 or 3 with each substrate (O_1 , O_2 , and AcOH) do not depend on the presence or absence of other coordinated substrates. The assumption of the absence of such influence seems quite reasonable for a big coordination centre such as a giant cluster with several hundred atoms of palladium.

A smaller value of the stability constant for the π -complex of the giant cluster with propylene as compared to ethylene may be explained by the size of the propylene molecule exceeding that of ethylene. Note that the surface of the cluster core is expected to be substantially screened by the bulky molecules of the phenanthroline ligand. Examination of the idealized structure of cluster 2 (Fig. 7) using molecular models shows that only *ca.* 20 palladium atoms on the surface of the metal skeleton of the cluster are sterically accessible for coordination of the olefin molecules. It may happen

that because of steric hindrance the more bulky C_3H_6 molecules will be coordinated at these sites more weakly than the smaller C_2H_4 .

For real molecules of giant clusters, with the structure probably deviating somewhat from the perfect polyhedron, the number of accessible coordination sites may deviate from that for the idealized model. The number of these sites can be determined experimentally using poisoning techniques, *i.e.* by carrying out the oxidation reaction in the presence of some ligands that can be strongly bound to those palladium atoms on the surface of the metal skeleton which are active in catalysis.

The data on the influence of different poisons on the rates of C_2H_4 and C_3H_6 oxidative acetoxylation in solutions of cluster 3 are presented in Fig. 15. These data show that the bulky ligands that coordinate well to Pd atoms, *e.g.* PPh_3 and phen, actually have no effect on the rate of the olefin oxidation, apparently because they cannot be coordinated on the sites suitable for olefin, O_2 and AcOH binding in the course of the reaction. The smaller ligands, *e.g.* C_2H_5SH and the thiocyanide anion, efficiently suppress the catalytic activity of the cluster. For complete inhibition of C_2H_4 oxidation, it is necessary to introduce *ca.* 50 ligand molecules to the surface of one cluster molecule, while for C_3H_6 oxidation, it is sufficient to introduce *ca.* 15 ligand molecules [38].

These data agree with the above supposition about the importance of steric requirements for the ability of a substrate molecule to form a complex with the giant cluster. Indeed about a three-fold decrease in the rate constant, k in eqn. (12) when passing from ethylene to propylene (Table 8), is shown by the poisoning experiments to result from a three-fold decrease in the number of the cluster surface sites available for coordination of the olefin molecule.

For further insight into the reaction mechanism, the kinetic isotope effects for C_2H_4 and C_3H_6 oxidative acetoxylation were studied. Table 9

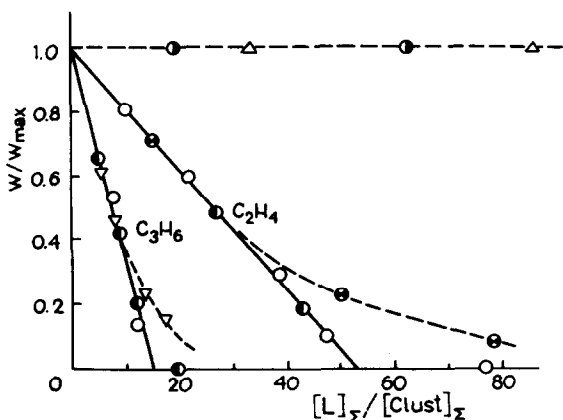


Fig. 15. The rates of the oxidative acetoxylation for propylene and ethylene, in MeCN-AcOH solution of cluster 3 as a function of the concentrations of ligand-inhibitors: (●) C_2H_5SH ; (▽) I_2 ; (○) Et_2NCS_2Na ; (⊙) $KSCN$; (△) phen; (⊖) PPh_3 .

TABLE 9

Kinetic isotope effects at 333 K

Substrate	Cluster	$k_{C_nH_{2n}}$	k_{CH_3COOH}
		$k_{C_nD_{2n}}$	k_{CD_3COOD}
ethylene	3	1.1 ± 0.1	1.1 ± 0.1
propylene	2	2.2 ± 0.2	1.0 ± 0.05
propylene	3	3.6 ± 0.2	1.0 ± 0.05
propylene	Pd black	1.0 ± 0.1	2.0 ± 0.2

contains the data on the influence of the substrate deuteration on the observed rate constant, k , of reactions (3) and (4).

Besides giant Pd clusters, two other types of species could also be suspected as responsible for catalytic activity in the oxidation of olefins by O_2 : (1) mononuclear Pd(II) complexes presumably arising from a giant cluster upon its dissociation; (2) particles of Pd metal, which could be formed as small impurities in reaction solutions upon the coalescence of clusters.

Assumption (1) can be, however, rejected on the basis of the above-mentioned differences in the reactivity of Pd clusters and mononuclear Pd(II) complexes.

Assumption (2) can also be rejected, since it is in contradiction with kinetic data. In particular, the difference in the kinetic isotope effects for propylene oxidation catalyzed by giant clusters and Pd black should be noted (Table 9).

Moreover, the oxidation of an equimolar mixture of ethylene and propylene in the presence of clusters 2 or 3 resulted in simultaneous formation of vinyl and allyl acetates in comparable quantities, while in the presence of Pd black, allyl acetate was formed as almost the sole product of the reaction.

In the light of these facts, it is reasonable to consider the observed olefin oxidation processes as catalyzed by giant cluster molecules rather than mononuclear Pd complexes or Pd metal particles.

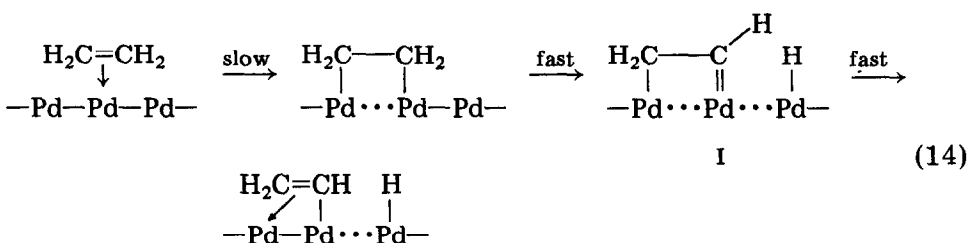
Mechanism of the oxidation of olefins. Besides the kinetic equations, the following three experimental facts are important for revealing the reaction mechanism:

(i) both ethylene and propylene are oxidized with nearly equal rate constants k in the presence of the same cluster 3, notwithstanding the pronounced difference between the C—H bond strengths in ethylene (vinyl—H, 445 ± 8 kJ) and in propylene (allyl—H, 362 ± 8 kJ) molecules [39].

(ii) The reaction of the oxidative acetoxylation of propylene in the presence of 2 and 3 yields only allyl acetate, no products of vinyl oxidation being observed at both low and high concentrations of all reacting species.

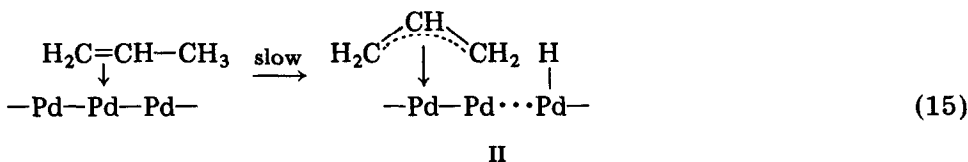
(iii) For ethylene oxidation, the kinetic isotope effects (KIE), within the limits of experimental error, are equal to unity both for ethylene and for acetic acid molecules. For propylene oxidation, KIE is equal to unity only for acetic acid, while for propylene it considerably exceeds this value (Table 9).

Different KIE observed upon deuteration of C_2H_4 and C_3H_6 (fact (iii)) suggest different rate-determining steps for the oxidative acetoxylation of these two olefins within the reaction Scheme 2. In the C_2H_4 molecule, the π -bond between two carbon atoms is the weakest (ca. 250 kJ). The data on KIE indicate (Table 9) that no transfer of H atoms from the coordinated C_2H_4 and CH_3COOH molecules occurs in the rate-determining stage. In this situation, we suggest that the rate-determining step might be an oxidative addition (with an opening the π -bond) of a π -coordinated C_2H_4 molecule to a Pd-Pd group of the cluster forming the σ, σ -coordinated $\cdot\cdot Pd-CH_2-CH_2-Pd\cdot\cdot$ group. Subsequent splitting of the C-H bond in this group is assumed to be fast and facilitated owing to the formation of the Pd=C multiple bond in the intermediate I [37]:



Similar species have been postulated as intermediates for hydrogenation, dehydrogenation, and H-D exchange of ethylene at the surfaces of noble metal catalysts [41, 42]. Evidence for formation of σ, σ -coordinated ethylene and π, σ -coordinated vinyl groups at the palladium(100) surface were recently obtained by the HREELS method [42].

In the case of propylene, the energy difference between the carbon-carbon π -bond and allyl-H bond is much less than the energy difference between carbon-carbon π -bond and vinyl-H bond in ethylene. Thus, the rate-determining step of the oxidative addition of a propylene molecule to a Pd-Pd group may include the splitting of the allyl-H bond, leading to the formation of the π -allyl complex and surface hydride:

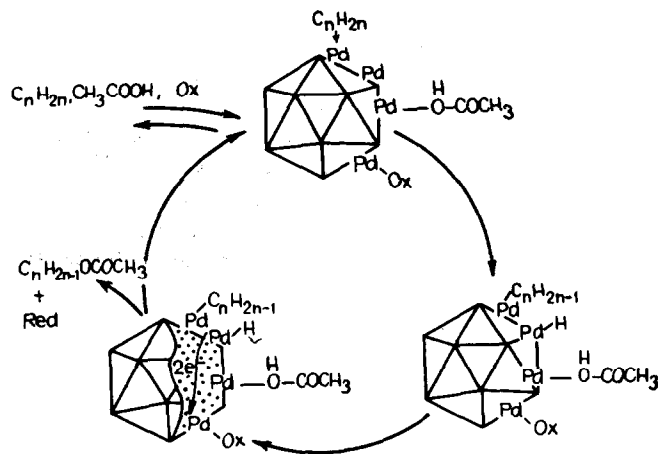


The splitting of the allyl-H bond in the rate-determining step explains a large KIE for oxidative acetoxylation of propylene (Table 9).

Formation of the surface π -allyl group in intermediate II appears to favour the 'allyl' direction of the reaction as compared to the 'vinyl'. Further reactions of vinyl or allyl groups and H atoms coordinated at the surface of the cluster metal skeleton are assumed to proceed rapidly and have no influence on the reaction rate.

The proposed mechanisms of olefin oxidative acetoxylation via reactions (14) and (15) indeed assume the rate-determining steps of this reaction to be different for ethylene and propylene. In this situation, the coincidence of the rate constants k for reactions of C_2H_4 and C_3H_6 (note that the observed *ca.* three-fold difference between the values of k in Table 8 has been shown to result mainly from different concentrations of sites for C_2H_4 and C_3H_6 coordination on the surface of the same cluster 3) must be considered as accidental, resulting from a chance coincidence of the free energies of activation for reaction (15) and the first step of reaction (14).

The data on inhibition of reactions (3) and (4) with poisoning ligands (Fig. 15) showed that only *ca.* 20% of the surface palladium atoms are available for reagent molecules in the oxidation of ethylene, and *ca.* 6% of these atoms in propylene oxidation. At the sterically screened surface, all three molecules (olefin, O_2 and AcOH) are barely coordinated to the neighbour palladium atoms at the same part of the cluster. It is more probable that a C_2H_4 or C_3H_6 molecule is initially bound at one site of the cluster surface, and an O_2 molecule at another site, not necessarily the neighbour to the site where the olefin molecule is located. In this situation, electron transfer from the Pd-alkenyl or Pd-H fragments to the coordinated O_2 molecule can perhaps occur through the metal skeleton, the latter acting as an 'electron mediator'. Thus, the general Scheme 3 can be assumed for the reaction of olefin acetoxylation over the giant Pd clusters, where $Ox = O_2$,

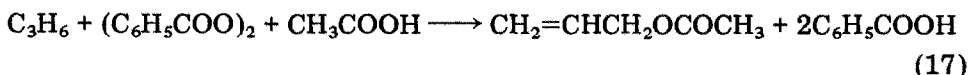


Scheme 3.

$(PhCOO)_2$ or Pd(II); Red = H_2O , PhCOOH or Pd(0), and reaction products $C_nH_{2n-1}OCOCH_3$ and Red are formed, respectively, upon recombination of

coordinated ($-C_nH_{2n-1}$), ($-OCOCH_3$) and ($-Ox$), ($-H$) species that collide during their migration over the surface of the cluster.

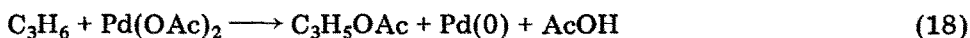
As is indicated in Scheme 3, other oxidants besides O_2 , *e.g.*, peroxides and Pd(II), can also serve as electron acceptors, in the cluster catalysis. For example, as we have found, benzoyl peroxide can be used as an electron acceptor in the presence of clusters 2 and 3 [43]. The reaction



proceeds in AcOH solution containing giant cluster 2 or 3, with 98 - 100% selectivity for allyl acetate, at 293 K and $10^{-3} - 10^{-4}$ M stationary concentration of benzoyl peroxide. Benzoyl peroxide must be introduced into the reaction solution in small portions to prevent the oxidation of the cluster. At higher concentrations of benzoyl peroxide, *e.g.*, $10^{-1} - 10^{-2}$ M, clusters 2 and 3 are oxidized to form Pd(II) complexes. If this occurs, ordinary homogeneous oxidation with Pd(II) proceeds, yielding a mixture of alkenyl acetates.

The reaction between C_3H_6 and benzoyl peroxides, producing only allyl acetate in high yield, can be also carried out in the presence of palladium black [43]. Under the same conditions, propylene was not oxidized by benzoyl peroxide in the absence of cluster 2 and 3 or Pd black. Therefore, reaction (17) may be regarded as a further example of the cluster-catalyzed oxidative acetoxylation of olefins, proceeding presumably via Scheme 3.

The approach based on Scheme 3 for catalysis with giant clusters may be applied also to the homogeneous oxidative acetoxylation of olefins under the action of Pd(II) in AcOH solutions, giving usually isopropenyl, *n*-propenyl and allyl acetates with comparable yields [35, 44]:



In the absence of additional oxidants, *e.g.* O_2 , dispersed metallic palladium particles formed as a product of reaction (18), are assumed to serve as a 'cluster' catalyst directing the oxidation process to an 'allyl route' via Scheme 3. This inference is supported by the curves of the product accumulations obtained in our experiments for the oxidation of propylene with $Pd(OAc)_2$ in an inert atmosphere (Fig. 16). These data show that the proportion of allyl acetate in the product mixture increases noticeably during the course of the reaction. The observed variation of the selectivity of the reaction towards formation of allyl acetate is thought to be caused by a competition between Pd(II) noncatalytic homogeneous and Pd 'cluster'-catalyzed heterogeneous reactions, the first yielding *n*-propenyl and isopropenyl acetates and the second one allyl acetate. From this point of view, the variations in selectivity of reaction (18) caused by changes of temperature, concentrations of AcONa and H_2O , etc., observed earlier in [35, 44] can be also realized in terms of Scheme 3, where a Pd metal particle acts as a 'cluster', and $Ox = Pd(OAc)_4^{2-}$. Finally, in the case where Pd(II) was absent, allyl acetate was found to be the sole product of

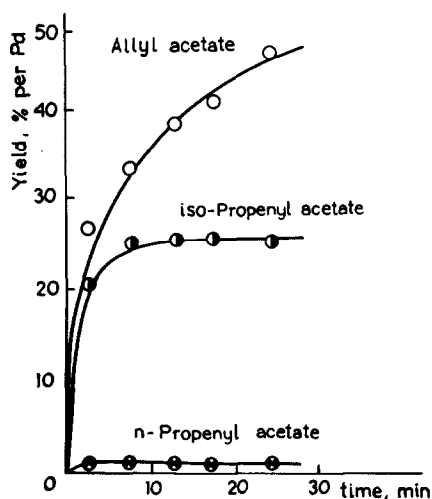


Fig. 16. Product accumulation in the course of the reaction between propylene and $\text{Pd}(\text{OAc})_2$ in AcOH solution containing 1.0 M NaOAc. 353 K, $[\text{Pd}]_0 = 5.0 \times 10^{-2}$ M.

propylene oxidative acetoxylation with dioxygen, catalyzed by Pd metal particles.

Acknowledgements

The authors thank Dr. V. M. Nekipelov, Dr. V. M. Mastikhin and Dr. V. D. Chinakov from the Institute of Catalysis, Academy of Sciences of the U.S.S.R., Siberian Branch (IC), and Dr. S. G. Sakharov and the Institute of General and Inorganic Chemistry, Academy of Sciences of the U.S.S.R. (IGIC), for aid in the NMR studies; Dr. V. M. Zaikovskiy from IC for aid in the electron microscopy experiments; Dr. A. N. Naumochkin from IC for aid in the EXAFS studies; Dr. V. N. Kolomyichuk from IC for the SAXS experiments; Dr. V. M. Novotortsev and Dr. O. G. Ellert from IGIC for the magnetic susceptibility measurements; Dr. G. I. Timofeeva from the Institute of Organo-Element Compounds of the Academy of Sciences of the U.S.S.R. (IOEC) for the aid in sedimentation experiments; Prof. Yu. T. Struchkov from IOEC for helpful discussions on cluster structures.

References

- 1 M. N. Vargaftik, V. P. Zagorodnikov, I. P. Stolarov, I. I. Moiseev, V. A. Likhobov, D. I. Kotchubey, A. L. Chuvilin, V. I. Zaikovskiy, K. I. Zamaraev and G. I. Timofeeva, *J. Chem. Soc., Chem. Commun.*, (1985) 937.
- 2 M. N. Vargaftik, V. P. Zagorodnikov, I. P. Stolarov, V. A. Likhobov, A. L. Chuvilin, V. I. Zaikovskiy, D. I. Kotchubey, G. I. Timofeeva, K. I. Zamaraev and I. I. Moiseev, *Dokl. Akad. Nauk SSSR*, 284 (1985) 896 (in Russ.).

- 3 (a) V. P. Zagorodnikov, M. N. Vargaftik, D. I. Kotchubey, A. L. Chuvilin, S. G. Sakharov, and M. A. Mayfat, *Izv. Akad. Nauk SSSR, Ser. Khim.*, (1986) 253 (in Russ.); (b) V. P. Zagorodnikov, M. N. Vargaftik, D. I. Kochubey, V. A. Likhobolov, V. N. Kolomiychuk, A. N. Naumochkin, A. L. Chuvilin, V. M. Novotortsev, O. G. Ellert and I. I. Moiseev, *Izv. Akad. Nauk SSSR, Ser. Khim.*, (1989) 849 (in Russ.).
- 4 M. N. Vargaftik, V. P. Zagorodnikov, I. P. Stolarov, D. I. Kochubey, V. M. Nekipelov, V. M. Mastikhin, V. D. Chinakov, K. I. Zamaraev and I. I. Moiseev, *Izv. Akad. Nauk SSSR, Ser. Khim.*, (1985) 2381 (in Russ.).
- 5 M. N. Vargaftik, V. P. Zagorodnikov and I. I. Moiseev, *Izv. Akad. Nauk SSSR, Ser. Khim.*, (1983) 1209 (in Russ.).
- 6 I. I. Moiseev, in A. E. Shilov (ed.), *Fundamental Research in Homogeneous Catalysis*, Vol. 4, Gordon and Breach, New York, London, 1986, p. 39.
- 7 (a) A. M. Vlasov, K. I. Zamaraev, M. A. Kozlov, D. I. Kochubey and M. A. Sheromov, *Khim. Fiz.*, 1 (1983) 663 (in Russ.); (b) K. I. Zamaraev and D. I. Kochubey, *Kinet. Katal.*, 27 (1986) 1031 (in Russ.).
- 8 B. K. Teo and P. A. Lee, *J. Am. Chem. Soc.*, 101 (1979) 2815.
- 9 D. I. Svergun, L. A. Feigin, *X-Ray and Neutron Small-Angle Scattering*, Nauka, Moscow (in Russ.), 1986.
- 10 G. Schmid, R. Pfeil, R. Boese, F. Bandermann, S. Meyer, G. H. M. Calis and J. W. A. van der Velden, *Chem. Ber.*, 114 (1981) 3634.
- 11 T. Shimidzu and M. Tamura, *Shokubai*, 16 (1974) 84.
- 12 S. Nakamura and T. Yasui, *J. Catal.*, 23 (1971) 315.
- 13 J. E. Lyons, G. Suld and Chao-Yang Hsu, in Yu Yermakov and V. Likhobolov (eds.), *Proc. Vth Int. Symp. Relations between Homogeneous and Heterogeneous Catalysis*, Novosibirsk, 1986, VNU Science Press, Utrecht, 1986, p. 117.
- 14 S. F. Polytsky, M. N. Vargaftik, A. M. Shkitov, I. P. Stolarov, I. I. Moiseev and O. M. Nefedov, *Izv. Akad. Nauk SSSR, Ser. Khim.*, (1978) 1913 (in Russ.).
- 15 M. N. Vargaftik, V. P. Zagorodnikov and I. I. Moiseev, *Kinet. Katal.*, 22 (1981) 951 (in Russ.).
- 16 I. P. Stolarov, M. N. Vargaftik, O. M. Nefedov and I. I. Moiseev, *Kinet. Katal.*, 23 (1982) 376 (in Russ.).
- 17 P. M. Maitlis, *The Organic Chemistry of Palladium*, Vol. 1, Academic Press, New York, 1971.
- 18 I. P. Stolarov, T. A. Stromnova, V. P. Zagorodnikov, M. N. Vargaftik, S. V. Zinchenko, V. A. Khutoryanskii, F. K. Schmidt and I. I. Moiseev, *Izv. Akad. Nauk SSSR, Ser. Khim.*, (1986) 942 (in Russ.).
- 19 V. P. Zagorodnikov, T. S. Khodashova, M. N. Vargaftik, I. I. Moiseev and M. A. Poray-Koshits, *Koord. Khim.*, 11 (1985) 95 (in Russ.).
- 20 A. I. Yanovskii, V. P. Zagorodnikov and Yu. T. Struchkov, *Koord. Khim.*, 12 (1986) 386 (in Russ.).
- 21 G. Schmid, *Structure and Bonding*, Vol. 62, Springer, Berlin-Heidelberg, 1985.
- 22 L. R. Wallenbert, J.-O. Bovin and G. Schmid, *Surf. Sci.*, 156 (1985) 256.
- 23 B. T. Heaton, P. Ingallina, R. Devenish, C. J. Humphreys, A. Ceriotti, G. Longoni and M. Marchionna, *J. Chem. Soc., Chem. Commun.*, (1987) 765.
- 24 B. K. Teo and N. J. A. Sloane, *Inorg. Chem.*, 24 (1985) 4545.
- 25 M. N. Vargaftik, T. A. Stromnova, T. S. Khodashova, M. A. Poray-Koshits and I. I. Moiseev, *Koord. Khim.*, 7 (1981) 132 (in Russ.).
- 26 E. G. Mednikov, N. K. Eremenko, Yu. L. Slovokhotov and Yu. T. Struchkov, *J. Chem. Soc., Chem. Commun.*, (1987) 218.
- 27 S. Ladas, B. R. A. Dalla Betta and M. Boudart, *J. Catal.*, 53 (1978) 356.
- 28 A. N. Naumochkin and D. I. Kochubey, *Nucl. Instruments and Methods in Physical Research*, A261 (1987) 163.
- 29 B. R. James, *Homogeneous Hydrogenation*, Wiley, New York, 1973.
- 30 V. P. Zagorodnikov and M. N. Vargaftik, *Izv. Akad. Nauk SSSR, Ser. Khim.* (1985) 2652 (in Russ.).

- 31 I. I. Moiseev, *π -Complexes in the Liquid-Phase Oxidation of Olefins*, Nauka, Moscow, 1970 (in Russ.).
- 33 I. I. Moiseev, *Advances in Science and Technology, Ser: Kinetics and Catalysts*, VINITI, Moscow, Vol. 13, 1984, p. 147 (in Russ.).
Moscow, Vol. 13, 1984, p. 147 (in Russ.).
- 34 M. K. Startchevsky, M. N. Vargaftik and I. I. Moiseev, *Kinet. Katal.*, 20 (1979) 1163 (in Russ.).
- 35 S. Winstein, J. McCaskie, H.-B. Lee and P. M. Henry, *J. Am. Chem. Soc.*, 98 (1976) 6913.
- 36 M. Tamura and T. Yasui, *Shokubai*, 21 (1979) 54.
- 37 V. P. Zagorodnikov and M. N. Vargaftik, *Kinet. Katal.*, 27 (1986) 851 (in Russ.).
- 38 I. P. Stolarov, M. N. Vargaftik and I. I. Moiseev, *Kinet. Katal.*, 28 (1987) 1359 (in Russ.).
- 39 V. N. Kondrat'ev, (ed.), *Chemical Bond Energies, Ionisation Potentials and Electron Affinities*, Nauka, Moscow, 1974, p. 39 (in Russ.).
- 40 I. Horiuti and M. Polanyi, *Trans. Faraday Soc.*, 30 (1934) 1164.
- 41 A. Farkas and L. Farkas, *J. Am. Chem. Soc.*, 60 (1938) 22.
- 42 E. M. Stuve and R. J. Madix, *J. Phys. Chem.*, 89 (1985) 105.
- 43 I. P. Stolarov, M. N. Vargaftik, O. M. Nefedov and I. I. Moiseev, *Izv. Akad. Nauk SSSR, Ser. Khim.*, (1983) 1455 (in Russ.).
- 44 I. I. Moiseev, A. P. Belov, V. A. Igoshin and Ya. K. Syrkin, *Dokl. Akad. Nauk SSSR*, 173 (1967) 863 (in Russ.).